Emergent strength-dependent scale-free mobility edge in a nonreciprocal long-range Aubry-André-Harper model

Gui-Juan Liu [1], Jia-Ming Zhang [1], Shan-Zhong Li [1,*] and Zhi Li [2,3,†]
[1] School of Physics, South China Normal University, Guangzhou 510006, China
[2] Key Laboratory of Atomic and Subatomic Structure and Quantum Control (Ministry of Education), Guangdong Basic Research Center of Excellence for Structure and Fundamental Interactions of Matter, School of Physics, South China Normal University, Guangzhou 510006, China
[3] Guangdong Provincial Key Laboratory of Quantum Engineering and Quantum Materials, Guangdong-Hong Kong Joint Laboratory of Quantum Matter, Frontier Research Institute for Physics, South China Normal University, Guangzhou 510006, China

(Received 27 March 2024; revised 30 May 2024; accepted 26 June 2024; published 22 July 2024)

We investigate the properties of the mobility edge in an Aubry-André-Harper model with nonreciprocal long-range hopping. The results reveal that there can be a type of mobility edge featuring both strength-dependent and scale-free properties. By calculating the fractal dimension, we find that the positions of mobility edges are robust to the strength of nonreciprocal long-range hopping. Furthermore, through scale analysis of the observables such as fractal dimension, eigenenergy, eigenstate, etc., we show that four different specific mobility edges can be observed in the system. This paper extends the family tree of mobility edges and hopefully it will shed more light on the related theory and experiment.

DOI: 10.1103/PhysRevA.110.012222

I. INTRODUCTION

In 1958, Anderson first proposed the famous localization theory. The theory tells us that strong random disorder will destroy the statistical physical ergodicity of electrons, which makes the corresponding wave function decay exponentially with space [1]. Anderson localization theory has drawn great attention in the past few decades because of not only the importance of the theory itself but also the fact that many new devices have been developed based on it. Nowadays, the study of localization theory has gradually extended from solid materials to more different systems, such as photonic crystal [2–4], waveguide array [5,6], circuit system [7], trapped ions [8], ultracold atomic gases [9–12], etc.

Then in 1970, scaling theory showed that an arbitrarily small disorder would lead to localization in a low-dimensional ($D < 3$) system [13,14]. In the three-dimensional case, the extended state and the localized state may coexist with an energy boundary, i.e., a mobility edge (ME), emerging between the two [15–17]. Past decades have seen great progress in the research on MEs. Researchers have come to know that MEs not only appear in random disordered systems but may also appear in quasiperiodic disordered systems [10,18–57]. Unlike random disordered systems, quasiperiodic systems are between order and disorder. Because quasiperiodic models are easy to deal with theoretically (some even have analytical solutions [18–26]), and easy to be realized experimentally [10,27–43], nowadays they have gotten ever-increasing attention. One of the most typical quasiperiodic models is the one-dimensional (1D) Aubry-André-Harper (AAH) chain, which possesses the property of self-duality [58]. Before (after) the critical point of phase transition, the system behaves as a pure extended phase (localized phase) without the emergence of a ME [58,59]. When the parameters are at the critical point, self-duality will work to ensure that real and reciprocal spaces have the same expression, and the corresponding eigenstates in the system exhibit the characteristics of multifractal states.

Furthermore, energy-dependent traditional MEs have been successfully induced in quasiperiodic AAH models by introducing long-range (LR) hopping [20,44,46], dimerized hopping [47,49], and modulating the quasiperiodic potential [22,26,41,50–57]], etc. In addition to the traditional ME of dividing extended states and localized states, new types of nontraditional MEs have also been explored in recent years. So far, it has been found that the introduction of p-wave superconductor pairing [60–64], quasiperiodic hopping [65–71], LR hopping [46,72–74] into the AAH model can induce the nontraditional ME involving multifractal states.

On the other hand, because of its excellent performance in describing dissipation or the nonequilibrium process, wide attention has been paid to the study of non-Hermitian properties [75–116]. Many new phenomena previously not found in Hermitian systems have been unveiled one after another [89,90]. The non-Hermitian skin effect of the nonreciprocal (NR) model, a typical phenomenon that only exists in non-Hermitian systems, has been extensively studied in recent years [91–116]. It has been noticed that the corresponding eigenstates in systems with the non-Hermitian skin effect are very sensitive to the boundary conditions [91].

So far, most of the research focuses on the AAH model with LR hopping or the non-Hermitian LR ordered model. More precisely, a recent study has reported that AAH models

*Contact author: shanzhongli88@gmail.com
†Contact author: lizphys@m.scnu.edu.cn

 ©2024 American Physical Society

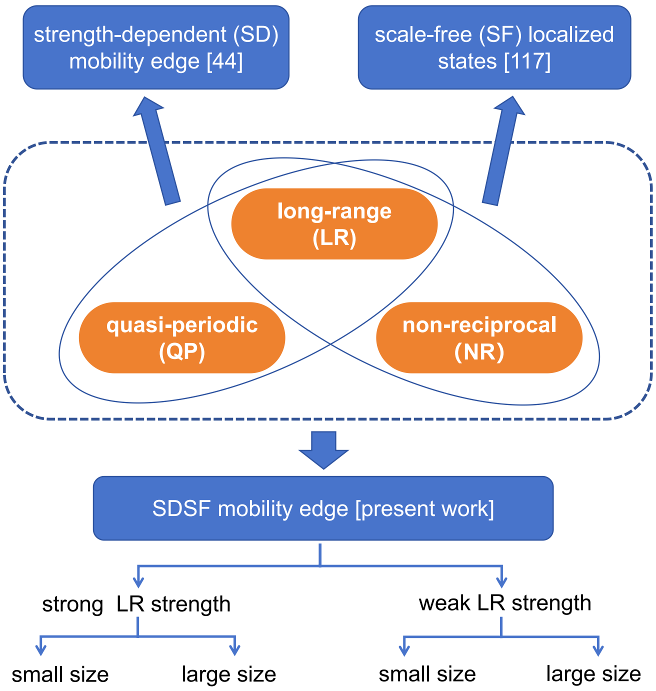

FIG. 1. The scheme for implementing strength-dependent scale-free MEs.

with LR hopping can produce a type of strength-dependent ME [44], while another study on non-Hermitian systems pointed out that nonreciprocal long-range (NRLR) hopping leads to the emergence of scale-free localized states in the system [117]. Scale-free localized states behave as skin states in small-size systems and extended states in large-size systems. Based on the above studies, it is natural to wonder whether there can be a ME featuring both strength-dependent and scale-free properties in an AAH model with NRLR hopping.

To answer this question, this paper is devoted to the study of the NRLR AAH model, and its results are shown in Fig. 1.

The rest of the paper is structured as follows. In Sec. II, we give a brief introduction to the theoretical model. In Secs. III and IV, we discuss properties of the system's ME with strong and weak LR hopping, respectively. The results of this paper and those in the Hermitian case are compared and analyzed in Sec. V. The experiment realization is discussed in Sec. VI. The main conclusions are summarized in Sec. VII.

II. MODEL

We start with a NRLR Aubry-André-Harper model. The corresponding Hamiltonian reads

$$H = H_{\mathrm{NRLR}} + H_{\mathrm{QP}},$$
$$H_{\mathrm{NRLR}} = \sum_{i<j} \frac{-J_L}{|i-j|^a} c_i^\dagger c_j + \sum_{i>j} \frac{-J_R}{|i-j|^a} c_j^\dagger c_i,$$
$$H_{\mathrm{QP}} = \sum_{j=1}^{L} \lambda \cos(2\pi\alpha j + \theta) c_j^\dagger c_j, \tag{1}$$

where H_{NRLR} and H_{QP} correspond to the NRLR hopping and the quasiperiodic potential, respectively. c_j $(c_j^\dagger)$ denotes the fermionic annihilation (creation) operator at site j, J_L (J_R) is the leftward (rightward) hopping strength, L is the system size, and a is the LR parameter, which determines the strength of LR hopping. The on-site potential is dominated by the quasiperiodic strength λ and the quasiperiodic parameter α, as well as the random phase θ. In the computing process, we set $\alpha = \lim_{v\to\infty} F_{v-1}/F_v = (\sqrt{5}-1)/2$, which can be obtained from the Fibonacci numbers $F_{v+1} = F_v + F_{v-1}$, where $F_0 = 0$ and $F_1 = 1$.

Without loss of generality, we fix $\theta = 0$ and set $J_L = 1$ as the unit of energy. When $J_R = 1$, the Hamiltonian reduces to the reciprocal Hermitian case [44]. In this case, both strong $(a < 1)$ and weak $(a > 1)$ LR hopping will cause a steplike phase transition from the P_1 phase to the P_4 phase with the increase of λ [see Figs. 2(a1) and 3(a1)]. The corresponding position of the ME appears at $P_s = \alpha^s L$, where $s = 1$, 2, 3, and 4 [44]. Under the condition of $a < 1$, the ME serves as a boundary to separate the extended state from the multifractal state, while under the condition of $a > 1$, it will separate the extended state from the localized state.

III. THE STRENGTH-DEPENDENT SCALE-FREE MOBILITY EDGE FOR THE CASE OF STRONG NRLR HOPPING: $a < 1$

The fractal dimension, as the key observable to judge the localization properties and phase transition of quasiperodic systems, is defined as [17,118–124]

$$\Gamma_\beta = -\lim_{L\to\infty} \frac{\ln \xi_\beta}{\ln L}, \tag{2}$$

where $\xi_\beta = \frac{\sum_{j=1}^{L} |\psi_{\beta,j}|^4}{[\sum_{j=1}^{L} |\psi_{\beta,j}|^2]^2}$ is the inverse participation ratio and $\psi_{\beta,j}$ is the amplitude at the j^{th} site for the β^{th} eigenstate. Γ approaches 1 and 0 for the extended and localized states, respectively, while $0 < \Gamma < 1$ for the multifractal states.

First, let us discuss the strong NRLR case $(a < 1)$. By fixing the parameter $a = 0.5$, we compute the fractal dimensions Γ of all eigenstates as a function of λ under the Hermitian $(J_R = 1)$ and the non-Hermitian $(J_R = 0.5)$ conditions, respectively [see Fig. 2(a)]. One can see clearly that MEs of both Hermitian and non-Hermitian cases exhibit a steplike transition from P_1 to P_4, resulting in a steplike change in the localization properties. Note that the fractal dimension Γ of the extended state decreases with the introduction of the non-Hermitian case; further discussion will show that this implies the emergence of a different type of state, i.e., the scale-free localized (SFL) state. To further illustrate the trend of the steplike phase transition, we calculate the average fractal dimension $\overline{\Gamma} = \frac{1}{L}\sum_{\beta=1}^{L} \Gamma_\beta$ and plot them in Fig. 2(b). The blue and red lines correspond to the Hermitian and non-Hermitian cases, respectively. The results show that for different values of λ, the fractal dimension $\overline{\Gamma}$ always decreases, and the gap between different phase regions (P_1-P_4) also narrows, which leads to the gradual flattening of the steplike phase transition.

Furthermore, we analyze the key quantities such as fractal dimensions, eigenvalues, and eigenstates under different system sizes by scaling theory. We choose $\lambda = 1.26$, which corresponds to the center of the P_2 region, to discuss the ME.

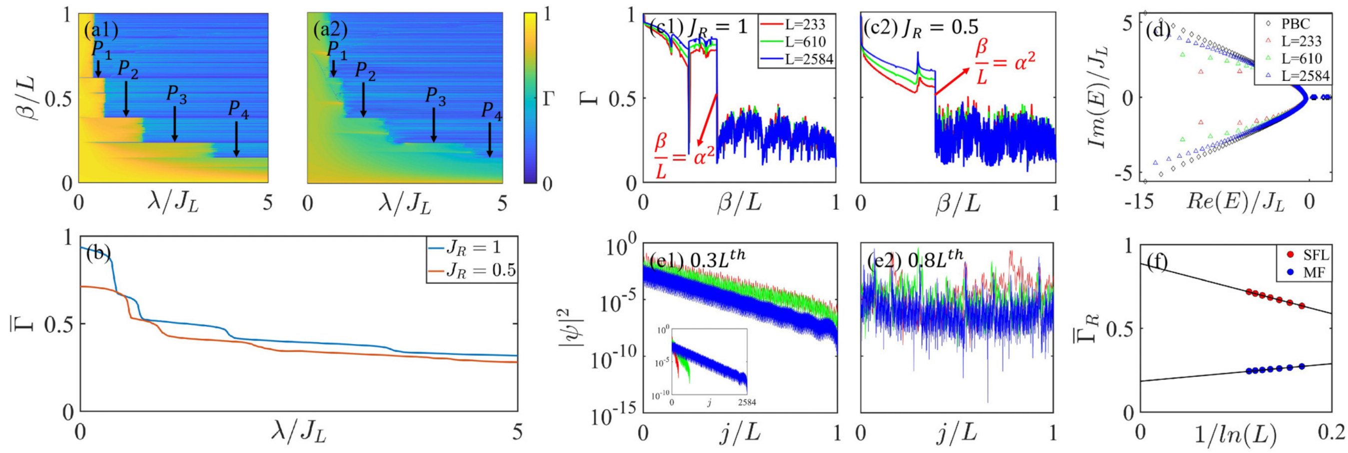

FIG. 2. The fractal dimension Γ of all eigenstates versus λ with $J_R = 1$ (a1) and $J_R = 0.5$ (a2). (b) The corresponding average fractal dimension $\overline{\Gamma}$. The scale effect of Γ with respect to the level index β/L at $\lambda = 1.26$ for $J_R = 1$ (c1) and $J_R = 0.5$ (c2). (d) The eigenenergy in the complex plane for different sizes with $\lambda = 1.26$, where the black diamond corresponds to PBCs with $L = 2584$. Panels (e1) and (e2) show the density distribution of the $0.3L^{\text{th}}$ and $0.8L^{\text{th}}$ eigenstates in log scale. Panel (f) shows the average fractal dimension $\overline{\Gamma}$ versus L for SFL and multifractal (MF) regions. The system size is $L = 610$ in panels (a1), (a2), and (b). Throughout, we set $a = 0.5$.

In Fig. 2(c), we plot the distribution of the fractal dimension in systems of different sizes. One can observe that for both Hermitian and non-Hermitian cases, Γ decreases abruptly at the energy index $\beta/L = \alpha^2 \approx 0.382$, suggesting that the NR hopping does not change the position of the ME. On the one hand, for the Hermitian limit ($J_R = 1$), one can find that, in the region $\beta/L < \alpha^2$, Γ tends to 1 with an increasing system size, suggesting that the region is extended [17]. Moreover, in the region $\beta/L > \alpha^2$, Γ is independent of system size, which indicates that the region is multifractal. This means, MEs of the Hermitian case are the boundary of extended states and multifractal states. On the other hand, for the NRLR case ($J_R = 0.5$), while the corresponding fractal dimension Γ in the region of $\beta/L < \alpha^2$ also increases with an increasing system size, the value magnitude of Γ becomes smaller than that of the Hermitian case. Through further analysis one can find that, in the region where $\beta/L > \alpha^2$, the fractal dimension Γ remains independent of system size, which means the corresponding eigenstates are the multifractal states.

In order to better show the system's localization properties and the difference between the open boundary condition (OBC) and the periodic boundary condition (PBC), we show the eigenvalues in the complex plane for different system sizes [see Fig. 2(d)]. One can find that the eigenvalues in the region of $\beta/L < \alpha^2$ depend on the system size and gradually converge to the case of the PBC. This is solid evidence of SFL states, where the eigenvalues of OBCs gradually converge to those of PBCs (or $L \to \infty$) [44]. In the region of $\beta/L > \alpha^2$, the corresponding eigenvalues, which are independent of the system size and boundary conditions, are always real. The scale-free property of the $\beta/L < \alpha^2$ region is also reflected in

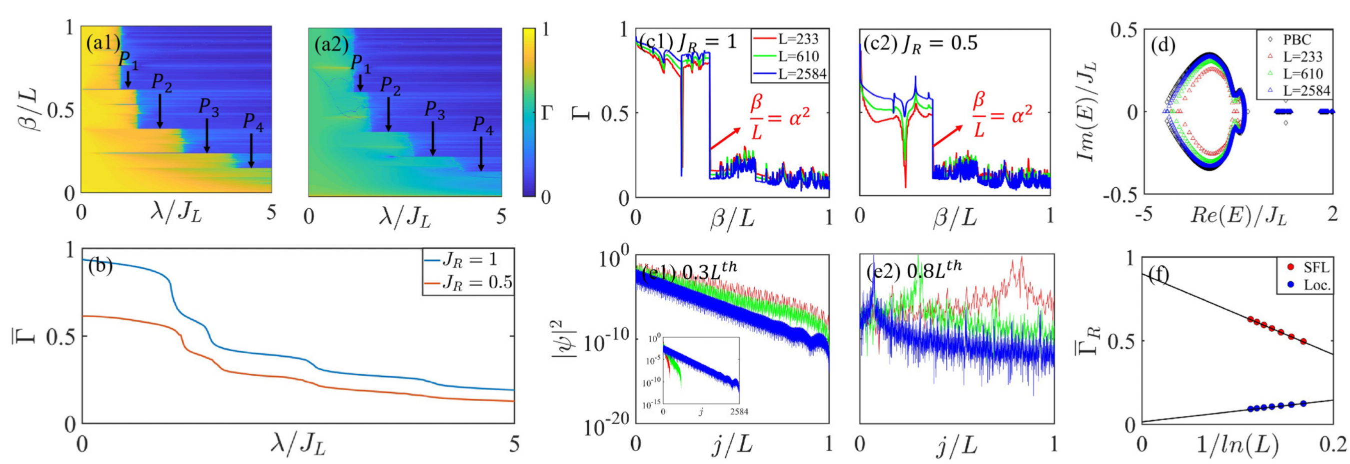

FIG. 3. The fractal dimension Γ of all eigenstates versus λ with $J_R = 1$ (a1) and $J_R = 0.5$ (a2). (b) The corresponding average fractal dimension $\overline{\Gamma}$. The scale effect of Γ with respect to the level index β/L at $\lambda = 2.08$ for $J_R = 1$ (c1) and $J_R = 0.5$ (c2). (d) The eigenenergy in the complex plane for different sizes with $\lambda = 2.08$, where the black diamond corresponds to PBCs with $L = 2584$. Panels (e1) and (e2) show the density distribution of the $0.3L^{\text{th}}$ and $0.8L^{\text{th}}$ eigenstates in log scale. Panel (f) is the average fractal dimension $\overline{\Gamma}$ versus L for SFL and localized (Loc.) regions. The system size is $L = 610$ in panels (a1), (a2), and (b). Throughout, we set $a = 1.5$.

the eigenstates [see Figs. 2(e1) and 2(e2)]. Figure 2(e1) shows the eigenstate corresponding to $\beta = 0.3L$. It can be seen that the corresponding wave function is exponentially localized at the left boundary in the case of small system size. Then, as the system size increases, the localization length will be protected, so that the distribution of the wave function will gradually be close to the extended state. Since SFL states exhibit an exponential profile $|\psi_j| \propto e^{-j\xi/L}$, where j is the site index, and ξ/L is the decay strength and is proportional to the system size L for arbitrary L, the rescaled probability profiles $L|\psi(j/L)|$ show the scale-invariant behavior [117]. Therefore, SFL states behave as skin states in small-size systems and as extended states in large-size systems. In other words, ξ/L will be smaller as the system size becomes larger. Although as shown in Fig. 2(e1), it seems that the larger the size is, the faster the decay is. However, that is actually not the case, for we normalize the system size. When the system size is not normalized, i.e., the horizontal axis directly uses the site index as shown in the inset in Fig. 2(e1), the distribution of the $0.3L^{\text{th}}$ eigenstate has a size-dependent localization length, and the eigenstate will become more and more extended as the system size increases, indicating the eigenstates in the region $\beta/L < \alpha^2$ are SFL states with size-dependent localization lengths. By a similar analysis, one can find that the eigenstates (the $0.8L^{\text{th}}$ eigenstate) remain multifractal in the multifractal region.

Since the system has well-defined MEs, one can define the average fractal dimension as

$$\overline{\Gamma}_R = \sum_R \frac{1}{L_R}\Gamma_R \tag{3}$$

for different regions to fit the thermodynamic limit, where $R =$ SFL or MF, which correspond to the eigenstates within the regions of $\beta/L < \alpha^2$ and $\beta/L > \alpha^2$, respectively. L_R is the total number of eigenstates in region R. As shown in Fig. 2(f), we find that the average fractal dimension $\overline{\Gamma}_R$ for the SFL region increases with an increasing L, eventually converging to about 0.9. While $\overline{\Gamma}_R$ does not strictly reach 1, it is sufficient to illustrate the extended properties of the region. In contrast, $\overline{\Gamma}_R$ in the multifractal region converges to a finite value. Therefore, the NRLR case for $a < 1$ exhibits the coexistence of extended and multifractal states under the condition of the thermodynamic limit. The MEs between them, which is the same to the Hermitian case, locate at $\beta_c/L = \alpha^2$ [44].

IV. THE SCALE-FREE MOBILITY EDGE FOR THE CASE OF WEAK NRLR: $a > 1$

Let us turn to the weak NRLR case ($a > 1$). Under such circumstances, the ME as the boundary separates the extended and localized states in the Hermitian case ($J_R = 1$) and also undergoes a transition from the P_1 phase to the P_4 phase with an increasing λ [44].

An analysis similar to that in the previous section is as follows. In Fig. 3(a) we show the fractal dimensions Γ versus λ for $J_R = 1$ and $J_R = 0.5$, and both cases exhibit steplike localization phase transitions. Similar to the case of $a = 0.5$, the non-Hermitian version does not change the position of the MEs. This implies that in the case $a > 1$ there will be another scale-free ME that separates SFL and Anderson localized states. In Fig. 3(b), we show the average fractal dimension $\overline{\Gamma}$ as a function of λ for different J_R values. Compared to the Hermitian case, $\overline{\Gamma}$ generally decreases, and the phase transition between different P_s phases becomes smoother.

Then, we fix $\lambda = 2.08$ (center of the P_2 region) to discuss the emergent scale-free ME. In Fig. 3(c), we show the Γ values of all eigenstates at different system sizes. In both Hermitian and non-Hermitian cases, the ME is at $\beta/L = \alpha^2$ and is not affected by NR hopping. For $J_R = 1$ [see Fig. 3(c1)], one can see that, in the region where $\beta/L < \alpha^2$, as the system size increases, Γ approaches 1, corresponding to extended states. In the region where $\beta/L > \alpha^2$, as the system size increases, Γ approaches 0, corresponding to localized states. This indicates that the MEs separate the extended and localized states. As shown in Fig. 3(c2), Γ increases with system size increasing in the region where $\beta/L < \alpha^2$. Similar to the case of $a = 0.5$, Γ remains small for finite sizes. Further scaling analysis reveals that the corresponding states are SFL states. In the region where $\beta/L > \alpha^2$, Γ approaches 0 as the system size increases, indicating that it is a localized region.

The scale-free properties of the $\beta/L < \alpha^2$ region can also be characterized by the eigenvalue and the distribution of the eigenstate. As shown in Fig. 3(d), one can see the gradual convergence of the eigenvalues in the $\beta/L < \alpha^2$ region to the PBC as the system size increases. The distribution of the $0.3L^{\text{th}}$ eigenstate has a size-dependent localization length [see Fig. 3(e1)], and the eigenstates will become more and more extended as the system size increases. For the region $\beta/L > \alpha^2$, as shown in Figs. 3(d) and 3(e2), both the eigenvalues and the eigenstates exhibit size-independent properties.

Finally, in Fig. 3(f) we conduct the scaling analysis of the average fractal dimension $\overline{\Gamma}_R$ of the two regions. The results reveal that by interpolating to the thermodynamic limit, $\overline{\Gamma}_R = 0$ for the localized region, while $\overline{\Gamma}_R$ approaches 1 for the SFL region, indicating the emergent scale-free ME that separates SFL states from Anderson localized states.

V. DISCUSSION

The main finding of this paper is a type of ME which depends on both system size and LR strength. The differences of MEs between the reciprocal LR case and the NRLR case are summarized in Table I.

For the Hermitian case, when the LR effect is strong (weak) $a < 1$ ($a > 1$) (see Appendix A), the MEs lie at the energy index $P_s = \alpha^s L$ separating the extended and multifractal (localized) states. Fortunately, the position formula obtained for the Hermitian case still holds for the non-Hermitian case. For the non-Hermitian case, the ME remains at the position of the energy indicator P_s. However, unlike the Hermitian version, the extended region will be replaced by the SFL state with a size-dependent localized length. To be more specific, when the system size is small, the SFL will localize on the boundary as a skin localized state. As the size increases the localization length increases (with a constant proportion of the system size), and eventually at system size infinity, it will become an extended state. Therefore, for $a < 1$ ($a > 1$), the ME will separate the SFL state and the multifractal (localized) state.

TABLE I. Comparison of mobility edges between reciprocal and nonreciprocal long-range AAH models.

	Reciprocal long-range AAH [44]		NRLR case (present work)			
Long-rang parameter:	$a < 1$	$a > 1$	$a < 1$		$a > 1$	
System size:	Independent of L		$L \ll \infty$	$L \to \infty$	$L \ll \infty$	$L \to \infty$
Mobility edge	Extended + multifractal	Extended + localized	Skin localized + multifractal	Extended + multifractal	Skin localized + localized	Extended + localized

VI. EXPERIMENT REALIZATION OF THE STRENGTH-DEPENDENT SCALE-FREE MOBILITY EDGE

Quantum simulators that can simulate AAH models, such as ultracold atoms [10,41,42], optical waveguide arrays [28–30], and superconducting circuits [39,43], can be considered as potential experimental platforms to realize the phenomena explored in this paper. We propose the experimental scheme for observing the SDSF mobility edge by taking the ultracold atomic gas as an example. So far, based on ^{87}Rb and ^{39}K atomic gases, the standard AAH model has been successfully realized in bichromatic optical lattices experiments [10,41,42]. In concrete terms, the first step is to cool down and obtain an ensemble of Bose-Einstein condensates in a harmonic trap. In the second step, the interaction among atoms is adjusted to 0 through the Feshbach resonance technique. Finally, the cold atoms are placed into a one-dimensional bichromatic optical lattice tube. By controlling the depth and energy ratios of the bichromatic lattice, the quasiperiodic potential and the hopping strength can be precisely adjusted.

In addition to the above experiment, it is also necessary to induce a long-range power-law hopping to realize the model in this paper. Experimentally, there are several ways to achieve long-range hopping in ultracold atomic lattice systems. For example, in a recent report, the dynamics of a one-dimensional Bose gas with power-law decaying hopping amplitudes was studied after an abrupt reduction of the hopping range [125–127]. After obtaining the AAH model with long-range hopping, the nonreciprocal hopping can be readily obtained by manipulating the auxiliary laser and, finally, the quantum simulation of the model discussed in this paper can be realized [75,76]. As for detection, it is necessary to detect the density distribution of the wave function under certain parameters by absorption imaging techniques. The phase of the system can be determined by the distribution of localized, extended, and skin states, etc., indicated by the density distribution.

VII. CONCLUSIONS

In conclusion, the ME properties of the 1D NRLR AAH model are explored in this paper. The rest of the phase diagram spanned by the exponent a and the hopping strength J_R is discussed in Appendix B. The results show that a type of scale-free ME can be induced by introducing the full-space NRLR hopping into the AAH model. In addition, we find that the NR effect has little effect on the position of the ME, but has a great effect on the phase segmented by the ME; i.e., the extended region corresponding to the Hermitian case can be transformed to the size-dependent SFL region. Since the SFL state has a size-dependent localization length, the wave function in the system exhibits properties of the skin localized state at small sizes but properties of the extended state at large sizes. This results in four different MEs in the system, namely, skin localized + multifractal, extended + multifractal, skin localized + localized, and extended + localized. Finally, several typical observables (such as the fractal dimension, eigenvalue, and eigen wave function of the system) are analyzed by scale theory, so as to show from different perspectives that the size-dependent ME does appear in the system.

ACKNOWLEDGMENTS

This work was supported by the Guangdong Basic and Applied Basic Research Foundation (Grant No. 2021A1515012350) and the National Key Research and Development Program of China (Grant No. 2022YFA1405300).

APPENDIX A: THE CRITICAL PROPERTIES OF $a = 1$

The conclusions come from Ref. [44], which provides a comprehensive exposition of the phase diagram of the long-range quasiperiodic model by numerical calculations, showing that $a < 1$ ($a > 1$) has mobility edges separating the extended state and the multifractal critical (localized) state. To show these conclusions more clearly, we have added corresponding descriptions of the critical characteristics of the system in the case of $a = 1$. To be more specific, we provide the energy spectrum to exhibit that the case $a = 1$ is truly the critical value (see Fig. 4).

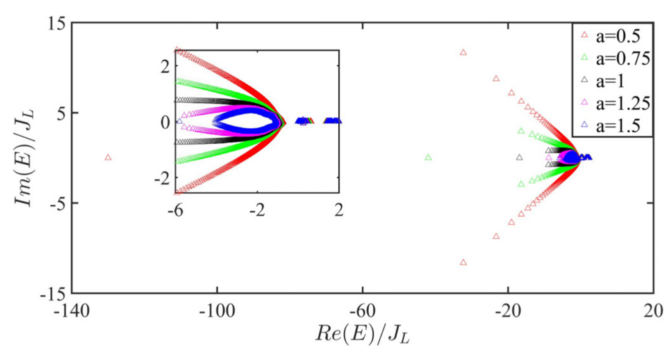

FIG. 4. Energy spectrum for different values of LR parameter a under PBCs with $L = 2584$. Throughout, we set $\lambda = 1.8$.

As shown in Fig. 4, in the case of $a > 1$, the energy spectrum in the complex plane will have a closed ringlike structure. That is to say, there will be two points of intersection with the real axis. In this case, the left intersection point will move in the negative direction as parameter a decreases. The position of the left intersection point will tend to $-\infty$ for the case of $a = 1$, which means there is only one intersection point left with the real axis in the energy spectrum and therefore the abovementioned closed ringlike structure cannot be produced. Note that, under the condition of $a > 1$, the imaginary part of the spectrum remains always a finite value. Then in the case of $a \leqslant 1$, the spectrum will take on a half-open structure, and the opening will become larger with the decrease of a. In this case, the imaginary part of the energy will gradually diverge rather than stay at a finite value, as shown in Fig. 4.

APPENDIX B: MORE DETAILS OF DIFFERENT PARAMETERS a AND J_R

We discuss the cases of different parameters a and the hopping strength J_R. As shown in Fig. 5, we exhibit Hermitian $J_R = J_L$ in Figs. 5(a1)–5(d1) and non-Hermitian $J_R \neq J_L$ in Figs. 5(a2)–5(d2).

The results are similar to those discussed in the main text, in that the introduction of the non-Hermitian case does not change the position of the mobility edge P_s, but makes the step transition between different P_s phases smooth. In addition, the fractal dimension of the eigenstates in the extended region decreases and transforms into SFL states under OBCs. When the parameter $a < 1$ ($a > 1$), the ME separates the skin states and multifractal (localized) states in small sizes and separates the extended states and multifractal (localized) states in large sizes.

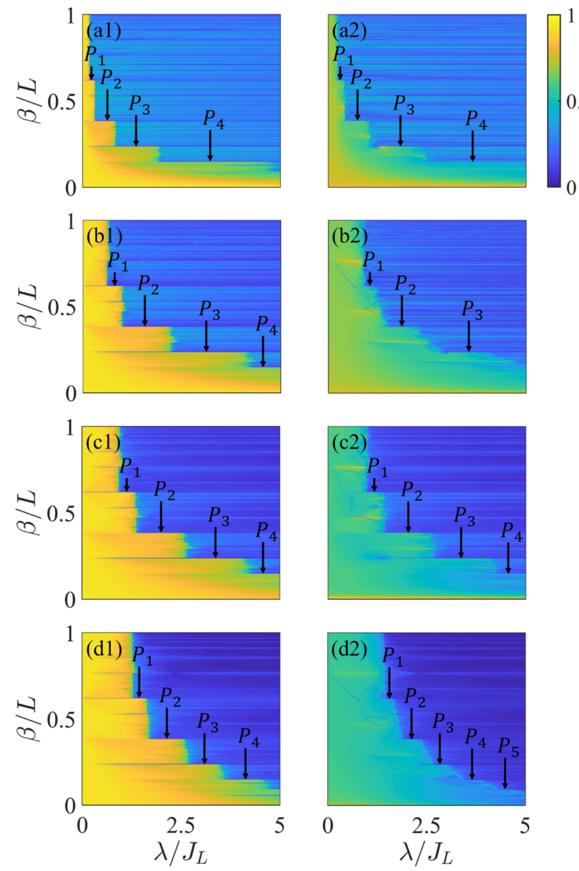

FIG. 5. (a) The fractal dimension Γ of all eigenstates versus λ when $a = 0.2$, $J_R = 1$ (a1); $a = 0.2$, $J_R = 0.8$ (a2); $a = 0.8$, $J_R = 1$ (b1); $a = 0.8$, $J_R = 0.2$ (b2); $a = 1.3$, $J_R = 1$ (c1); $a = 1.3$, $J_R = 0.8$ (c2); $a = 2$, $J_R = 1$ (d1); and $a = 2$, $J_R = 0.2$ (d2). Throughout, we set $L = 610$.

[1] P. W. Anderson, Absence of diffusion in certain random lattices, Phys. Rev. **109**, 1492 (1958).

[2] M. Störzer, P. Gross, C. M. Aegerter, and G. Maret, Observation of the critical regime near Anderson localization of light, Phys. Rev. Lett. **96**, 063904 (2006).

[3] T. Schwartz, G. Bartal, S. Fishman, and M. Segev, Transport and Anderson localization in disordered two-dimensional photonic lattices, Nature (London) **446**, 52 (2007).

[4] J. Topolancik, B. Ilic, and F. Vollmer, Experimental observation of strong photon localization in disordered photonic crystal waveguides, Phys. Rev. Lett. **99**, 253901 (2007).

[5] Y. Lahini, Y. Bromberg, D. N. Christodoulides, and Y. Silberberg, Quantum correlations in two-particle Anderson localization, Phys. Rev. Lett. **105**, 163905 (2010).

[6] C. Thompson, G. Vemuri, and G. S. Agarwal, Anderson localization with second quantized fields in a coupled array of waveguides, Phys. Rev. A **82**, 053805 (2010).

[7] S. Pai, M. Pretko, and R. M. Nandkishore, Localization in fractonic random circuits, Phys. Rev. X **9**, 021003 (2019).

[8] A. Bermudez, M. A. Martin-Delgado, and D. Porras, The localization of phonons in ion traps with controlled quantum disorder, New J. Phys. **12**, 123016 (2010).

[9] J. Billy, V. Josse, Z. Zuo, A. Bernard, B. Hambrecht, P. Lugan, D. Clément, L. Sanchez-Palencia, P. Bouyer, and A. Aspect, Direct observation of Anderson localization of matter waves in a controlled disorder, Nature (London) **453**, 891 (2008).

[10] G. Roati, C. D'Errico, L. Fallani, M. Fattori, C. Fort, M. Zaccanti, G. Modugno, M. Modugno and M. Inguscio, Anderson localization of a non-interacting Bose–Einstein condensate, Nature (London) **453**, 895 (2008).

[11] A. Aspect and M. Inguscio, Anderson localization of ultracold atoms, Phys. Today **62**(8), 30 (2009).

[12] D. H. White, T. A. Haase, D. J. Brown, M. D. Hoogerland, M. S. Najafabadi, J. L. Helm, C. Gies, D. Schumayer, and D. A. W. Hutchinson, Observation of two-dimensional Anderson localisation of ultracold atoms, Nat. Commun. **11**, 4942 (2020).

[13] E. Abrahams, P. W. Anderson, D. C. Licciardello, and T. V. Ramakrishnan, Scaling theory of localization: Absence of quantum diffusion in two dimensions, Phys. Rev. Lett. **42**, 673 (1979).

[14] B. Hetényi, S. Parlak, and M. Yahyavi, Scaling and renormalization in the modern theory of polarization: Application to disordered systems, Phys. Rev. B **104**, 214207 (2021).

[15] N. F. Mott, Electrons in disordered structures, Adv. Phys. **16**, 49 (1967).

[16] P. A. Lee and T. V. Ramakrishnan, Disordered electronic systems, Rev. Mod. Phys. **57**, 287 (1985).

[17] F. Evers and A. D. Mirlin, Anderson transitions, Rev. Mod. Phys. **80**, 1355 (2008).

[18] S. Das Sarma, S. He, and X. C. Xie, Mobility edge in a model one-dimensional potential, Phys. Rev. Lett. **61**, 2144 (1988).

[19] S. Das Sarma, S. He, and X. C. Xie, Localization, mobility edges, and metal-insulator transition in a class of one-dimensional slowly varying deterministic potentials, Phys. Rev. B **41**, 5544 (1990).

[20] J. Biddle and S. Das Sarma, Predicted mobility edges in one-dimensional incommensurate optical lattices: An exactly solvable model of Anderson localization, Phys. Rev. Lett. **104**, 070601 (2010).

[21] S. Longhi, Metal-insulator phase transition in a non-Hermitian Aubry-André-Harper model, Phys. Rev. B **100**, 125157 (2019).

[22] Y. Wang, X. Xia, L. Zhang, H. Yao, S. Chen, J. You, Q. Zhou, and X.-J. Liu, One-dimensional quasiperiodic mosaic lattice with exact mobility edges, Phys. Rev. Lett. **125**, 196604 (2020).

[23] S. Longhi, Non-Hermitian Maryland model, Phys. Rev. B **103**, 224206 (2021).

[24] T. Liu and X. Xia, Real-complex transition driven by quasiperiodicity: A class of non-$\mathcal{PT}$ symmetric models, Phys. Rev. B **105**, 054201 (2022).

[25] X. Xia, K. Huang, S. Wang, and X. Li, Exact mobility edges in the non-Hermitian t_1-t_2 model: Theory and possible experimental realizations, Phys. Rev. B **105**, 014207 (2022).

[26] S. Ganeshan, J. H. Pixley, and S. Das Sarma, Nearest neighbor tight binding models with an exact mobility edge in one dimension, Phys. Rev. Lett. **114**, 146601 (2015).

[27] J. Koo, L. R. Walker, and S. Geschwind, Anderson localization and mobility edges in ruby, Phys. Rev. Lett. **35**, 1669 (1975).

[28] S. A. Gredeskul and Y. S. Kivshar, Generation of dark solitons in optical fibers, Phys. Rev. Lett. **62**, 977 (1989).

[29] D. N. Christodoulides and Y. Silberberg, Discretizing light behaviour in linear and nonlinear waveguide lattices, Nature (London) **424**, 817 (2003).

[30] T. Pertsch, U. Peschel, J. Kobelke, K. Schuster, H. Bartelt, S. Nolte, A. Tünnermann, and F. Lederer, Nonlinearity and disorder in fiber arrays, Phys. Rev. Lett. **93**, 053901 (2004).

[31] Y. Lahini, R. Pugatch, F. Pozzi, M. Sorel, R. Morandotti, N. Davidson, and Y. Silberberg, Observation of a localization transition in quasiperiodic photonic lattices, Phys. Rev. Lett. **103**, 013901 (2009).

[32] G. Modugno, Anderson localization in Bose-Einstein condensates, Rep. Prog. Phys. **73**, 102401 (2010).

[33] Y. E. Kraus, Y. Lahini, Z. Ringel, M. Verbin, and O. Zilberberg, Topological states and adiabatic pumping in quasicrystals, Phys. Rev. Lett. **109**, 106402 (2012).

[34] M. Verbin, O. Zilberberg, Y. E. Kraus, Y. Lahini, and Y. Silberberg, Observation of topological phase transitions in photonic quasicrystals, Phys. Rev. Lett. **110**, 076403 (2013).

[35] D. Tanese, E. Gurevich, F. Baboux, T. Jacqmin, A. Lemaître, E. Galopin, I. Sagnes, A. Amo, J. Bloch, and E. Akkermans, Fractal energy spectrum of a polariton gas in a fibonacci quasiperiodic potential, Phys. Rev. Lett. **112**, 146404 (2014).

[36] M. Verbin, O. Zilberberg, Y. Lahini, Y. E. Kraus, and Y. Silberberg, Topological pumping over a photonic Fibonacci quasicrystal, Phys. Rev. B **91**, 064201 (2015).

[37] M. Lohse, C. Schweizer, O. Zilberberg, M. Aidelsburger, and I. Bloch, A Thouless quantum pump with ultracold bosonic atoms in an optical superlattice, Nat. Phys. **12**, 350 (2016).

[38] S. Nakajima, T. Tomita, S. Taie, T. Ichinose, H. Ozawa, L. Wang, M. Troyer, and Y. Takahashi, Topological Thouless pumping of ultracold fermions, Nat. Phys. **12**, 296 (2016).

[39] P. Roushan, C. Neill, J. Tangpanitanon, V. M. Bastidas, A. Megrant, R. Barends, Y. Chen, Z. Chen, B. Chiaro, A. Dunsworth, A. Fowler, B. Foxen, M. Giustina, E. Jeffrey, J. Kelly, E. Lucero, J. Mutus, M. Neeley, C. Quintana, D. Sank *et al.*, Spectroscopic signatures of localization with interacting photons in superconducting qubits, Science **358**, 1175 (2017).

[40] F. A. An, E. J. Meier, and B. Gadway, Engineering a flux-dependent mobility edge in disordered zigzag chains, Phys. Rev. X **8**, 031045 (2018).

[41] H. P. Lüschen, S. Scherg, T. Kohlert, M. Schreiber, P. Bordia, X. Li, S. Das Sarma, and I. Bloch, Single-particle mobility edge in a one-dimensional quasiperiodic optical lattice, Phys. Rev. Lett. **120**, 160404 (2018).

[42] M. Schreiber, S. S. Hodgman, P. Bordia, H. P. Lüschen, M. H. Fischer, R. Vosk, E. Altman, U. Schneider, and I. Bloch, Observation of many-body localization of interacting fermions in a quasirandom optical lattice, Science **349**, 842 (2015).

[43] H. Li, Y.-Y. Wang, Y.-H. Shi, K. Huang, X. Song, G.-H. Liang, Z.-Y. Mei, B. Zhou, H. Zhang, J.-C Zhang, S. Chen, S.-P. Zhao, Y. Tian, Z.-Y Yang, Z. Xiang, K. Xu, D. Zheng, and H. Fan, Observation of critical phase transition in a generalized Aubry-André-Harper model with superconducting circuits, npj Quantum Inf. **9**, 40 (2023).

[44] X. Deng, S. Ray, S. Sinha, G. V. Shlyapnikov, and L. Santos, One-dimensional quasicrystals with power-law hopping, Phys. Rev. Lett. **123**, 025301 (2019).

[45] P. Wang, Y. Zheng, X. Chen, C. Huang, Y. V. Kartashov, L. Torner, V. V. Konotop, and F. Ye, Localization and delocalization of light in photonic moiré lattices, Nature (London) **577**, 42 (2020).

[46] N. Roy and A. Sharma, Fraction of delocalized eigenstates in the long-range Aubry-André-Harper model, Phys. Rev. B **103**, 075124 (2021).

[47] S. Roy, T. Mishra, B. Tanatar, and S. Basu, Reentrant localization transition in a quasiperiodic chain, Phys. Rev. Lett. **126**, 106803 (2021).

[48] F. A. An, K. Padavić, E. J. Meier, S. Hegde, S. Ganeshan, J. H. Pixley, S. Vishveshwara, and B. Gadway, Interactions and mobility edges: observing the generalized Aubry-André model, Phys. Rev. Lett. **126**, 040603 (2021).

[49] W. Han and L. Zhou, Dimerization-induced mobility edges and multiple reentrant localization transitions in non-Hermitian quasicrystals, Phys. Rev. B **105**, 054204 (2022).

[50] X. Li, X. Li, and S. Das Sarma, Mobility edges in one-dimensional bichromatic incommensurate potentials, Phys. Rev. B **96**, 085119 (2017).

[51] H. Yao, H. Khouldi, L. Bresque, and L. Sanchez-Palencia, Critical behavior and fractality in shallow one-dimensional quasiperiodic potentials, Phys. Rev. Lett. **123**, 070405 (2019).

[52] V. Goblot, A. Štrkalj, N. Pernet, J. L. Lado, C. Dorow, A. Lemaître, L. L. Gratiet, A. Harouri, I. Sagnes, S. Ravets,

A. Amo, J. Bloch, and O. Zilberberg, Emergence of criticality through a cascade of delocalization transitions in quasiperiodic chains, Nat. Phys. **16**, 832 (2020).
[53] T. Liu, H. Guo, Y. Pu, and S. Longhi, Generalized Aubry-André self-duality and mobility edges in non-Hermitian quasiperiodic lattices, Phys. Rev. B **102**, 024205 (2020).
[54] A. Štrkalj, E. V. H. Doggen, I. V. Gornyi, and O. Zilberberg, Many-body localization in the interpolating Aubry-André-Fibonacci model, Phys. Rev. Res. **3**, 033257 (2021).
[55] L.-J. Zhai, G.-Y. Huang, and S. Yin, Cascade of the delocalization transition in a non-Hermitian interpolating Aubry-André-Fibonacci chain, Phys. Rev. B **104**, 014202 (2021).
[56] A. Padhan, M. K. Giri, S. Mondal, and T. Mishra, Emergence of multiple localization transitions in a one-dimensional quasiperiodic lattice, Phys. Rev. B **105**, L220201 (2022).
[57] S.-Z. Li and Z. Li, The multiple re-entrant localization in a phase-shift quasiperiodic chain, arXiv:2305.12321.
[58] S. Aubry and G. André, Analyticity breaking and Anderson localization in incommensurate lattices, Ann. Israel Phys. Soc. **3**, 18 (1980).
[59] S. Y. Jitomirskaya, Metal-insulator transition for the almost Mathieu operator, Ann. Math. **3**, 150 (1999).
[60] J. Wang, X.-J. Liu, G. Xianlong, and H. Hu, Phase diagram of a non-Abelian Aubry-André-Harper model with *p*-wave superfluidity, Phys. Rev. B **93**, 104504 (2016).
[61] M. Yahyavi, B. Hetényi, and B. Tanatar, Generalized Aubry-André-Harper model with modulated hopping and *p*-wave pairing, Phys. Rev. B **100**, 064202 (2019).
[62] T. Liu, S. Cheng, H. Guo, and G. Xianlong, Fate of Majorana zero modes, exact location of critical states, and unconventional real-complex transition in non-Hermitian quasiperiodic lattices, Phys. Rev. B **103**, 104203 (2021).
[63] J. Fraxanet, U. Bhattacharya, T. Grass, M. Lewenstein, and A. Dauphin, Localization and multifractal properties of the long-range Kitaev chain in the presence of an Aubry-André-Harper modulation, Phys. Rev. B **106**, 024204 (2022).
[64] S.-Z. Li, and Z. Li, Emergent recurrent extension phase transition in a quasiperiodic chain, arXiv:2304.11811.
[65] F. Liu, S. Ghosh, and Y. D. Chong, Localization and adiabatic pumping in a generalized Aubry-André-Harper model, Phys. Rev. B **91**, 014108 (2015).
[66] J. C. C. Cestari, A. Foerster, and M. A. Gusmão, Fate of topological states in incommensurate generalized Aubry-André models, Phys. Rev. B **93**, 205441 (2016).
[67] L. Wang, N. Liu, S. Chen, and Y. Zhang, Quantum walks in the commensurate off-diagonal Aubry-André-Harper model, Phys. Rev. A **95**, 013619 (2017).
[68] T. Xiao, D. Xie, Z. Dong, T. Chen, W. Yi, and B. Yan, Observation of topological phase with critical localization in a quasi-periodic lattice, Sci. Bull. **66**, 2175 (2021).
[69] T. Liu and X. Xia, Dual mapping and quantum criticality in quasiperiodic Su-Schrieffer-Heeger chains, Phys. Rev. B **104**, 134202 (2021).
[70] L.-Z. Tang, G.-Q. Zhang, L.-F. Zhang, and D.-W. Zhang, Localization and topological transitions in non-Hermitian quasiperiodic lattices, Phys. Rev. A **103**, 033325 (2021).
[71] X.-C. Zhou, Y. Wang, T.-F. J. Poon, Q. Zhou, and X.-J. Liu, Exact new mobility edges between critical and localized states, Phys. Rev. Lett. **131**, 176401 (2023).
[72] Z. Xu, X. Xia, and S. Chen, Non-Hermitian Aubry-André model with power-law hopping, Phys. Rev. B **104**, 224204 (2021).
[73] D. Peng, S. Cheng, and G. Xianlong, Power law hopping of single particles in one-dimensional non-Hermitian quasicrystals, Phys. Rev. B **107**, 174205 (2023).
[74] M. Gonçalves, B. Amorim, E. V. Castro, and P. Ribeiro, Critical phase dualities in 1D exactly solvable quasiperiodic models, Phys. Rev. Lett. **131**, 186303 (2023).
[75] Z. Gong, Y. Ashida, K. Kawabata, K. Takasan, S. Higashikawa, and M. Ueda, Topological phases of non-Hermitian systems, Phys. Rev. X **8**, 031079 (2018).
[76] F. Song, S. Yao, and Z. Wang, Non-Hermitian skin effect and chiral damping in open quantum systems, Phys. Rev. Lett. **123**, 170401 (2019).
[77] C. H. Lee, L. Li, and J. Gong, Hybrid higher-order skin-topological modes in non-reciprocal systems, Phys. Rev. Lett. **123**, 016805 (2019).
[78] Z. Yang, K. Zhang, C. Fang, and J. Hu, Non-Hermitian bulk-boundary correspondence and auxiliary generalized Brillouin zone theory, Phys. Rev. Lett. **125**, 226402 (2020).
[79] Y. Liu, X.-P. Jiang, J. Cao, and S. Chen, Non-Hermitian mobility edges in one-dimensional quasicrystals with parity-time symmetry, Phys. Rev. B **101**, 174205 (2020).
[80] D.-W. Zhang, L.-Z. Tang, L.-J. Lang, H. Yan, and S.-L. Zhu, Non-Hermitian topological Anderson insulators, Sci. China: Phys., Mech. Astron. **63**, 267062 (2020).
[81] D.-W. Zhang, Y.-L. Chen, G.-Q. Zhang, L.-J. Lang, Z. Li, and S.-L. Zhu, Skin superfluid, topological Mott insulators, and asymmetric dynamics in an interacting non-Hermitian Aubry-André-Harper model, Phys. Rev. B **101**, 235150 (2020).
[82] L.-J. Zhai, S. Yin, and G.-Y. Huang, Many-body localization in a non-Hermitian quasiperiodic system, Phys. Rev. B **102**, 064206 (2020).
[83] L.-J. Zhai, G.-Y. Huang, and S. Yin, Nonequilibrium dynamics of the localization-delocalization transition in the non-Hermitian Aubry-André model, Phys. Rev. B **106**, 014204 (2022).
[84] L.-J. Lang, S.-L. Zhu, and Y. D. Chong, Non-Hermitian topological end breathers, Phys. Rev. B **104**, L020303 (2021).
[85] Z.-X. Guo, X.-J. Yu, X.-D. Hu, and Z. Li, Emergent phase transitions in a cluster Ising model with dissipation, Phys. Rev. A **105**, 053311 (2022).
[86] H.-Z. Li, X.-J. Yu, and J.-X. Zhong, Non-Hermitian Stark many-body localization, Phys. Rev. A **108**, 043301 (2023).
[87] S.-Z. Li, X.-J. Yu, and Z. Li, Emergent entanglement phase transitions in non-Hermitian Aubry-André-Harper chains, Phys. Rev. B **109**, 024306 (2024).
[88] X.-J. Yu, Z. Pan, L. Xu, and Z.-X. Li, Non-Hermitian strongly interacting Dirac fermions, Phys. Rev. Lett. **132**, 116503 (2024).
[89] E. J. Bergholtz, J. C. Budich, and F. K. Kunst, Exceptional topology of non-Hermitian systems, Rev. Mod. Phys. **93**, 015005 (2021).
[90] X. Zhang, T. Zhang, M. H. Lu, and Y. F. Chen, A review on non-Hermitian skin effect, arXiv:2205.08037.
[91] S. Yao and Z. Wang, Edge states and topological invariants of non-Hermitian systems, Phys. Rev. Lett. **121**, 086803 (2018).
[92] V. M. Martinez Alvarez, J. E. Barrios Vargas, and L. E. F. Foa Torres, Non-Hermitian robust edge states in one

dimension: Anomalous localization and eigenspace condensation at exceptional points, Phys. Rev. B **97**, 121401(R) (2018).

[93] F. K. Kunst, E. Edvardsson, J. C. Budich, and E. J. Bergholtz, Biorthogonal bulk-boundary correspondence in non-Hermitian systems, Phys. Rev. Lett. **121**, 026808 (2018).

[94] K. Yokomizo and S. Murakami, Non-Bloch band theory of non-Hermitian systems, Phys. Rev. Lett. **123**, 066404 (2019).

[95] C. H. Lee and R. Thomale, Anatomy of skin modes and topology in non-Hermitian systems, Phys. Rev. B **99**, 201103(R) (2019).

[96] H. Jiang, L.-J. Lang, C. Yang, S.-L. Zhu, and S. Chen, Interplay of non-Hermitian skin effects and Anderson localization in nonreciprocal quasiperiodic lattices, Phys. Rev. B **100**, 054301 (2019).

[97] S. Longhi, Probing non-Hermitian skin effect and non-Bloch phase transitions, Phys. Rev. Res. **1**, 023013 (2019).

[98] D. S. Borgnia, A. J. Kruchkov, and R.-J. Slager, Non-Hermitian boundary modes and topology, Phys. Rev. Lett. **124**, 056802 (2020).

[99] N. Okuma, K. Kawabata, K. Shiozaki, and M. Sato, Topological origin of non-Hermitian skin effects, Phys. Rev. Lett. **124**, 086801 (2020).

[100] K. Zhang, Z. Yang, and C. Fang, Correspondence between winding numbers and skin modes in non-Hermitian systems, Phys. Rev. Lett. **125**, 126402 (2020).

[101] K. Kawabata, N. Okuma, and M. Sato, Non-Bloch band theory of non-Hermitian Hamiltonians in the symplectic class, Phys. Rev. B **101**, 195147 (2020).

[102] A. Ghatak, M. Brandenbourger, J. van Wezel, and C. Coulais, Observation of non-Hermitian topology and its bulk-edge correspondence in an active mechanical metamaterial, Proc. Natl. Acad. Sci. USA **117**, 29561 (2020).

[103] S. Weidemann, M. Kremer, T. Helbig, T. Hofmann, A. Stegmaier, M. Greiter, R. Thomale, and A. Szameit, Topological funneling of light, Science **368**, 311 (2020).

[104] L. Xiao, T. Deng, K. Wang, G. Zhu, Z. Wang, W. Yi, and P. Xue, Non-Hermitian bulk-boundary correspondence in quantum dynamics, Nat. Phys. **16**, 761 (2020).

[105] C. Scheibner, W. T. M. Irvine, and V. Vitelli, Non-Hermitian band topology and skin modes in active elastic media, Phys. Rev. Lett. **125**, 118001 (2020).

[106] T. Helbig, T. Hofmann, S. Imhof, M. Abdelghany, T. Kiessling, L. W. Molenkamp, C. H. Lee, A. Szameit, M. Greiter, and R. Thomale, Generalized bulk-boundary correspondence in non-Hermitian topolectrical circuits, Nat. Phys. **16**, 747 (2020).

[107] Y. Yi and Z. Yang, Non-Hermitian skin modes induced by on-site dissipations and chiral tunneling effect, Phys. Rev. Lett. **125**, 186802 (2020).

[108] L. Li, C. H. Lee, S. Mu, and J. Gong, Critical non-Hermitian skin effect, Nat. Commun. **11**, 5491 (2020).

[109] L. Xiao, T. Deng, K. Wang, Z. Wang, W. Yi, and P. Xue, Observation of non-Bloch parity-time symmetry and exceptional points, Phys. Rev. Lett. **126**, 230402 (2021).

[110] L. Li, C. H. Lee, and J. Gong, Impurity induced scale-free localization, Commun. Phys. **4**, 42 (2021).

[111] Q. Lin, T. Li, L. Xiao, K. Wang, W. Yi, and P. Xue, Observation of non-Hermitian topological Anderson insulator in quantum dynamics, Nat. Commun. **13**, 3229 (2022).

[112] K. Zhang, Z. Yang, and C. Fang, Universal non-Hermitian skin effect in two and higher dimensions, Nat. Commun. **13**, 2496 (2022).

[113] Q. Liang, D. Xie, Z. Dong, H. Li, H. Li, B. Gadway, W. Yi, and B. Yan, Dynamic signatures of non-Hermitian skin effect and topology in ultracold atoms, Phys. Rev. Lett. **129**, 070401 (2022).

[114] Q. Lin, T. Li, L. Xiao, K. Wang, W. Yi, and P. Xue, Topological phase transitions and mobility edges in non-Hermitian quasicrystals, Phys. Rev. Lett. **129**, 113601 (2022).

[115] B. Li, H.-R. Wang, F. Song, and Z. Wang, Scale-free localization and $\mathcal{PT}$ symmetry breaking from local non-Hermiticity, Phys. Rev. B **108**, L161409 (2023).

[116] C.-X. Guo, X. Wang, H. Hu, and S. Chen, Accumulation of scale-free localized states induced by local non-Hermiticity, Phys. Rev. B **107**, 134121 (2023).

[117] Y.-C. Wang, H. H. Jen, and J.-S. You, Scaling laws for non-Hermitian skin effect with long-range couplings, Phys. Rev. B **108**, 085418 (2023).

[118] F. Wegner, Inverse participation ratio in $2+\varepsilon$ dimensions, Z. Phys. B **36**, 209 (1980).

[119] H. Aoki, Critical behaviour of extended states in disordered systems, J. Phys. C **16**, L205 (1983).

[120] H. Aoki, Fractal dimensionality of wave functions at the mobility edge: Quantum fractal in the Landau levels, Phys. Rev. B **33**, 7310 (1986).

[121] M. Janssen, Statistics and scaling in disordered mesoscopic electron systems, Phys. Rep. **295**, 1 (1998).

[122] A. D. Mirlin, Y. V. Fyodorov, A. Mildenberger, and F. Evers, Exact relations between multifractal exponents at the Anderson transition, Phys. Rev. Lett. **97**, 046803 (2006).

[123] A. De Luca, B. L. Altshuler, V. E. Kravtsov, and A. Scardicchio, Anderson localization on the Bethe lattice: Nonergodicity of extended states, Phys. Rev. Lett. **113**, 046806 (2014).

[124] X. Deng, B. L. Altshuler, G. V. Shlyapnikov, and L. Santos, Quantum levy flights and multifractality of dipolar excitations in a random system, Phys. Rev. Lett. **117**, 020401 (2016).

[125] W. S. Dias, D. Bertrand, and M. L. Lyra, Bose-Einstein condensation in chains with power-law hoppings: Exact mapping on the critical behavior in d-dimensional regular lattices, Phys. Rev. E **95**, 062105 (2017).

[126] P. Richerme, Z.-X. Gong, A. Lee, C. Senko, J. Smith, M. Foss-Feig, S. Michalakis, A. V. Gorshkov, and C. Monroe, Non-local propagation of correlations in quantum systems with long-range interactions, Nature (London) **511**, 198 (2014).

[127] P. Jurcevic, B. P. Lanyon, P. Hauke, C. Hempel, P. Zoller, R. Blatt, and C. F. Roos, Quasiparticle engineering and entanglement propagation in a quantum many-body system, Nature (London) **511**, 202 (2014).